Identification of the Transfer Function in a Model Gas Turbine Combustor : Application to Active Control of Combustion Instabilities

D. Bernier, S. Ducruix, F. Lacas*, S. Candel
Laboratoire EM2C, CNRS, Ecole Centrale Paris 92295 Châtenay Malabry, France
francois@em2c.ecp.fr
N. Robart, T. Poinsot
IMFT, Avenue du professeur Camille Soula 31400 Toulouse, France

Key words : System Identification, Active Control, Combustion Instabilities, Swirl, Gas Turbine.

1 Introduction

Dynamical phenomena leading to instability are often observed in modern lean premixed combustors. Because these oscillations are not easily suppressed by standard methods, active control constitutes a possible alternative. Closed-loop controllers for combustion instabilities are based on a time-delay scheme. This is however limited to a narrow domain of operation. A more sophisticated controller applies different gain and phase at each frequency depending on the system to control. Such controllers need to model the system behaviour through an identification step. We present here an experimental study of identification process in the case of a swirl stabilized spray combustor. The measured transfer function is used in the active control of combustion instabilities.

2 Experimental set-up

The experiments are performed in a laboratory scale Lean Premixed Prevaporized (LPP) atmospheric combustor operating at a heat release of 70 kW. The general description of the test rig may be found in Ref. [1]. The fuel-air premixing system (Fig. 1) is similar to an industrial gas turbine LPP injector. The swirl number at the exit of the injector is $S = 0.22$.

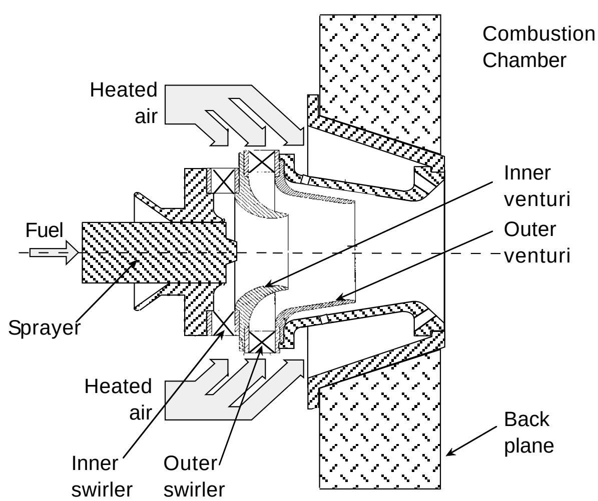

Figure 1: Sketch of the LPP injector

*Corresponding author

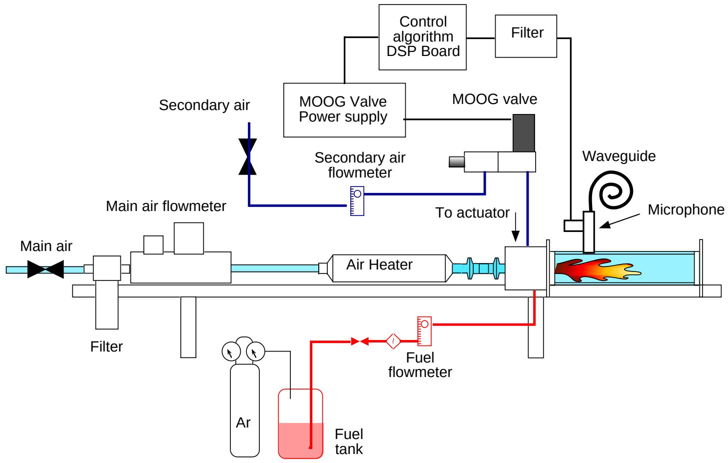

Figure 2: Sketch of the experimental set-up including closed-loop control set-up

An overview of the set-up is shown in Fig. 2. The burner is supplied with electrically preheated air at 600 K. Air flow rate is kept constant at 22 g s^{-1}. Liquid heptane is used as fuel with a flow rate of 1.4 g s^{-1}. The mixture equivalence ratio is $\Phi = 0.9$. The combustion chamber is 50 cm long with a square section of 10×10 cm^2. Lateral fused silica windows allow optical access. A plug located on the upper wall of the combustor at 5.5 cm from its entry is used for unsteady pressure measurements with a microphone mounted on a wave guide.

The actuator consists of secondary air injection. This airflow is separated into four high speed air jets before impacting the fuel spray at its basis (Fig. 3). The modulation of airflow rate is obtained with a MOOG electromagnetic valve designed for high frequency response (up to 400 Hz). The instantaneous equivalence ratio fluctuates while the mean equivalence ratio is kept constant with or without actuation. The mean airflow rate through the actuator is 1.0 g s^{-1} which corresponds to 4 % of the total airflow in the burner.

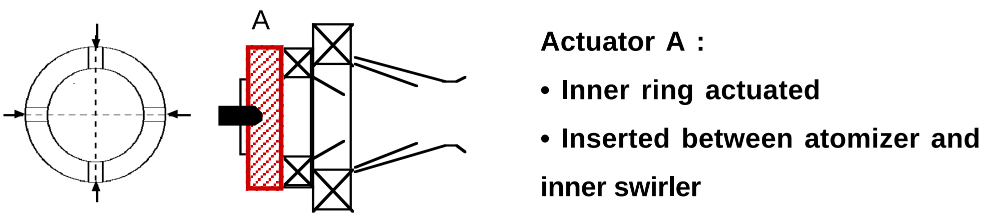

Figure 3: Sketch of the actuator

The overview of the set-up for closed-loop control is sketched in Fig. 2. A microphone detects the instability and transmits the measured signal to a low-pass filter. The filtered signal is then transmitted to the controller. The low-pass filtering operated at 1 kHz eliminates higher frequency disturbances. The sampling frequency on the DS1102 dSPACE board is 5 kHz. A threshold and an offset are applied to the output signal of the controller to fit the driving requirements of the high speed valve.

3 Control algorithm

A noise source semi-adaptive algorithm is used to control combustion instabilities. The controller is described in detail in Ref. [2,3] and presented in Fig. 4. The system is modelled by a finite impulse response

(FIR) numerical filter with 200 coefficients. The coefficients of the controller are optimized to reduce the oscillations through a modified LMS algorithm which inputs are the system model and the microphone signal. The algorithm minimizes the energy for actuation as soon as the oscillation level is reduced.
The FIR filter defines the behaviour of the system comprised between output and input of the controller. This includes actuation and injection systems, combustion chamber, sensor and low-pass filter. The FIR filter is defined by series of coefficients a_i. The pressure $y(t)$ at instant t can be predicted by :

$$y(t) = \sum_{i=1}^{N} a_i \, x(t - i\,\Delta t) \tag{1}$$

where $x(t)$ is the control algorithm output, Δt the sampling period and N the FIR filter order.
The estimation of the system behaviour is carried out during the identification step via open-loop white noise injection (Fig. 4) before the control itself. Identification converges in about 10 s. Since the instabilities in the burner occur around 400 Hz, the white noise used for identification is filtered at 800 Hz.

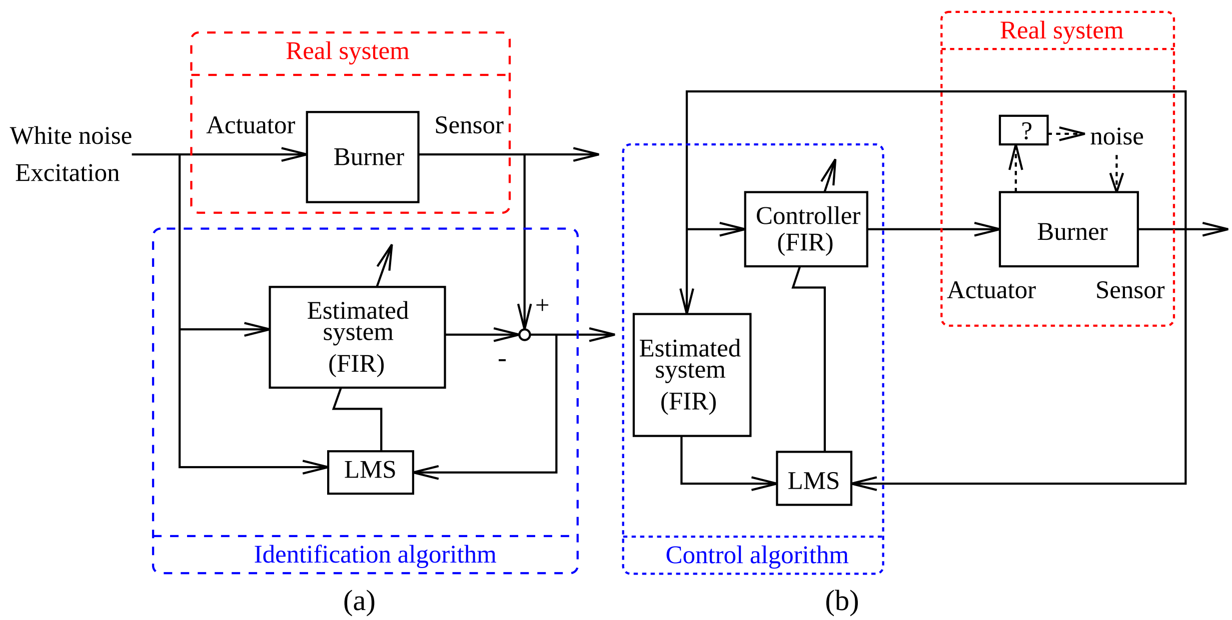

Figure 4: Sketches : (a) Off-line system identification algorithm (b) Noise-source semi-adaptive controller

The updating scheme of both identification and control are carried out via a LMS algorithm. A leakage factor is introduced in the basic algorithm for controller optimization. The leak provides the necessary spectral content for control convergence [4]. The modified updating algorithm for the controller is given by :

$$\mathbf{w}_{k+1} = \nu\, \mathbf{w}_k + \mu\, \mathbf{e'}_k\, e_k \tag{2}$$

with $0 < \nu < 1$. If $\nu = 1$, the original update law without leak is obtained. The vector containing the filter coefficients to update is denoted as $\mathbf{w}$, e is the error signal delivered by the microphone and $\mathbf{e'}$ denotes the filtered error signal in vector form. The index k designates the discrete time instants.
The cost function to be minimized by the leaky LMS algorithm is given by :

$$\hat{\xi} = e_k^2 \tag{3}$$

where e_k^2 corresponds to the squared instantaneous error signal.

4 Results

One can compute a direct transfer function between the valve command and the microphone pressure signals. The secondary path estimated during the identification process is supposed to model the same transfer function. Both transfer functions are plotted in Fig. 5, in the form of amplitude and phase as a function of frequency. The same figure shows the difference between the two transfer functions. One may see that both determination techniques are in good agreement for frequencies below $f_c = 420\,\mathrm{Hz}$. Coherence between command and pressure signals is strongly decreasing beyond f_c corresponding to the electro-valve bandwidth. The system behaviour is well reproduced in the pertinent frequency range.

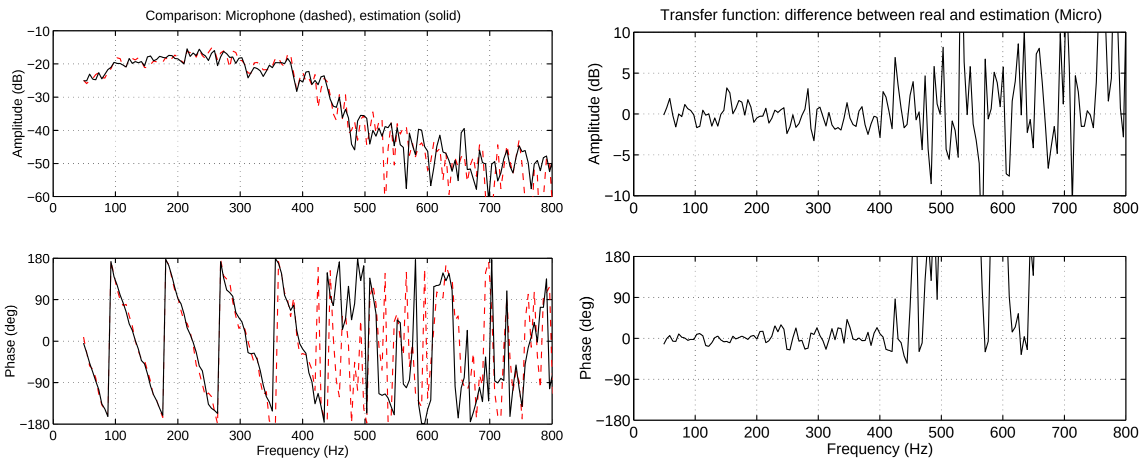

Figure 5: Transfer function of the burner (left hand-side). Comparison between estimation via FIR numerical filter and measurements from real signals (valve command and microphone signals). Difference between real and estimation (right hand-side)

A sensitive parameter that should be precisely reproduced is the phase of the transfer function. Indeed, an error greater than 90° on the phase may lead to a divergence during control operation. The difference between estimation and real transfer function in the burner is shown on the right part in Fig. 5. The error in phase is $\Delta\phi < 40°$ for frequencies lower than $f < 420\,\mathrm{Hz}$. For instability frequencies below 400 Hz, the precision on the phase is adequate. The estimated transfer function of the secondary path is accurate enough to allow closed-loop control using this model in the algorithm.
An example of transition between unstable and controlled mode in the swirl stabilized combustor is presented on the left part in Fig. 6. A transition between controlled and unstable mode is presented on the right part. The plots show microphone and electro-valve command signals during both transitions. The electro-valve command signal is rapidly increasing once the controller has been switched on. Simultaneously, the pressure signal amplitude is decreasing. From the average over series of ten tests, this process takes approximately $\tau \sim 70\,\mathrm{ms}$. Then, once the microphone signal reaches its controlled amplitude, the command signal is decreasing, optimizing the energy level required by the controller. One may notice that the controller effectiveness is not perfect. Some limited duration pressure bursts are observed during the control phase.
The same unstable/controlled transition has been observed for ten cases in the same regime, so that mean values of pressure oscillations reduction could be measured. The semi-adaptive noise-source controller can reduce the root mean squared (rms) pressure in the combustor from $p_u = 650\,\mathrm{Pa}$ in the unstable case to $p_c = 400\,\mathrm{Pa}$ in the controlled situation. Considering the mean pressure level $p_{st} = 130\,\mathrm{Pa}$ under stable operation, one can define a control efficiency as the reduction of pressure level due to unstable combustion as $R = (p_u - p_c) / (p_u - p_{st})$. The mean efficiency value in the studied regime is $R = 50\,\%$.

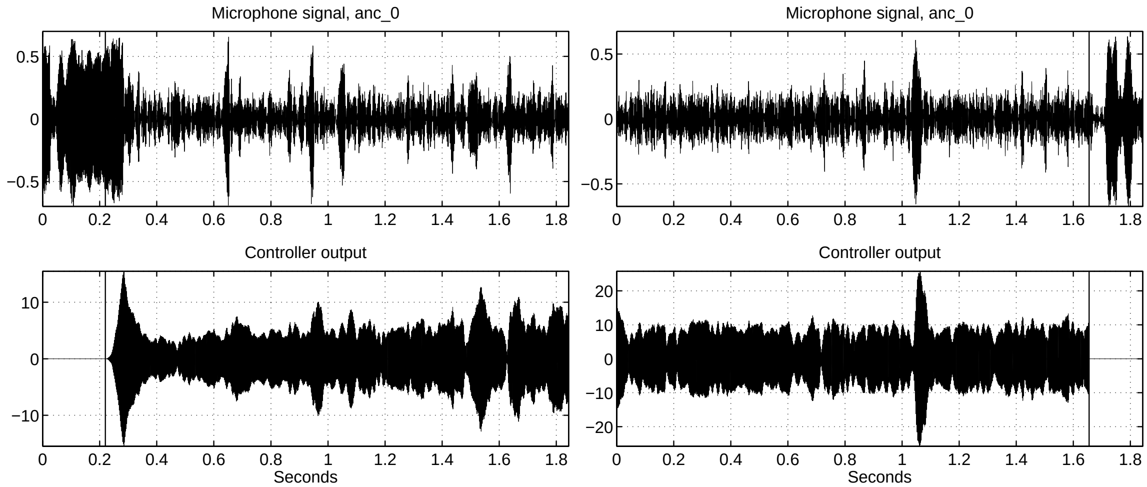

Figure 6: Microphone signal (upper plot) and controller ouput signal (lower plot). On the left, the controller is switched on at vertical line. On the right, the controller is switched off at vertical line.

5 Conclusion

A system identification method is used to determine accurate estimates of the transfer function in the case of a swirl stabilized spray combustor operating at 70 kW. The error in phase on the estimated transfer function is below 40° in the frequency range of interest while a difference greater than 90° would lead to controller divergence. The model could be integrated in a noise source semi-adaptive controller. The algorithm could reduce the oscillations level due to unstable combustion by 50 %. The next step is to integrate the method in a self-adaptive controller where the system identification is performed simultaneously with control.

Acknowledgements

Support for this research has been provided by the european community in the frame of the Brite Euram contract ACIACOC (BE97-4324).

References

[1] D. Bernier, F. Lacas, and S. Candel. Instability mechanisms in a lean premixed prevaporized combustor. *Submitted to Journal of Propulsion and Power*, 2001.

[2] M. Mettenleiter, E. Haile, and S. Candel. Adaptive control of aeroacoustic instabilities with application to propulsion systems. In *RTO AVT Symposium*, number 39 in RTO MP-14, Lisbon, 1998.

[3] M. Mettenleiter, E. Haile, and S. Candel. Adaptive control of aeroacoustic instabilities. *Journal of Sound and Vibration*, 230(4):761–789, 2000.

[4] S. M. Kuo and D. R. Morgan. *Active noise control systems*. John Wiley & Sons, 1996.